



## Classification of Raw EEG Motor Imagery Signals with Improved Convolutional Neural Networks for Use in Brain-Computer Interfaces

Dr. K. Padmavathi<sup>1</sup>, P. Divya<sup>2</sup>, M. Snehateja<sup>3</sup>, B. Srikanth<sup>4</sup>

<sup>1,2,3,4</sup>

Associate professor, Dept. of ECE, Indur Institute of Engg. & Tech., Siddipet, Telangana, India.

**Email ID:** padmaengineer@gmail.com<sup>1</sup>, divya.padakanti419@gmail.com<sup>2</sup>, snehateja666@gmail.com<sup>3</sup>, srikanth409@gmail.com<sup>4</sup>

### Abstract

The EEG motor imagery-based brain-computer interface (BCI) has drawn an interest from neuro-engineering researchers and is currently being utilized in various rehabilitative contexts. The performance of BCI systems may be negatively impacted by EEG motor imagery with a very low signal to noise ratio. This paper presents a novel technique for classifying EEG motor imagery, which is based on a continuous neural network and an improved convolutional neural network. The utilization of a continuous wavelet transforms incorporating three distinct mother wavelets enables the capture of a comprehensive EEG image through the amalgamation of time-frequency and electrode location. The purpose of this work is to reduce the computational complexity of a convolutional neural network while increasing its recognition of motor imagery tasks. The BCI competition IV dataset 2b was used to verify the suggested approach. The findings prove that the suggested methods outperform the current ones in terms of classification performance, making a brain-computer interface based on motor imagery a real possibility.

**Keywords:** Brain-computer interface, convolution neural network, dual-channel, electroencephalography, motor imagery.

### 1. Introduction

The acquisition and processing of brain signals in a number of offline or online ways are what make brain-computer interfaces (BCI) possible. Brain signals are gathered using techniques like positron emission tomography (PET), magnetoencephalography (MEG), electrocorticography (ECoG), electroencephalography (EEG), near-infrared spectral imaging (NIRS), functional magnetic resonance imaging (fMRI), and local field potentials and action potentials [1-4]. Various signal processing methods are used to extract the unique characteristics of the gathered signals. These distinct features are classified and linked up to a device that performs the intended function, where they are either integrated into a control system or employed as a control signal. Several researchers have recently investigated the utilization of convolutional neural networks for the purpose of extracting EEG signals. This approach aims to reduce the number of connections and parameters in a deep network by leveraging advantageous geographical or temporal associations

among adjacent data points to deduce favorable characteristics for a given machine learning task. The authors Yang et al. (2019) introduced a method called frequency complementary map selection (FCMS) that utilizes augmented CSP (ACSP) to mitigate the reliance of feature mapping on frequency bands in convolutional neural networks (CNNs). Nevertheless, this approach fails to fully utilize the temporal information provided by EEG. In their study, Tabar et al. [6] employed the Short-time Fourier transformation (STFT) technique to convert EEG signals into image signals. These image signals were subsequently subjected to classification using Convolutional Neural Networks (CNN) and automatic stacking encoding (SAE). Xu et al. [7] trained a deep transfer convolution neural network on the MI dataset to classify EEG signals. Compared to support vector machines (SVM), artificial neural networks (ANN), and conventional CNN, it was found to be more effective and accurate. In order to interpret the features learned by an EEG-based BCI, Lawhern et al. [8] proposed EEGNet and employed a

compact convolutional neural network. They also showed three methods for visualizing the contents of a trained EEGNet model. Dai et al. [9] purposefully constructed several convolution kernel scales for EEG signals in different frequency bands, and one-dimensional convolution kernels are used to perform convolution operations in the temporal and spatial dimensions. It was found that samples with identical labels are segmented, swapped, and recombined; samples are then separated into frequency bands, and segments within the same band are switched and recombined. Input signals were processed using a CSP filter by Majidov and Whangbo [10], who also evaluated the power spectral density (PSD) of each frequency band and added a particle swarm optimization approach to optimize features. The supplied application was analyzed using a CNN with a single convolutional layer. Using a hybrid network and the Filter Bank Common Spatial Pattern algorithm, Zhang et al. [11] extracted multimodal characteristics with improved outcomes over previous methods. Ma et al. [12] used a sliding window to improve the data and computed the peak-to-average power ratio (PSR) for suitable frequency ranges. Convolution kernels of size 3 by 3 were used to divide the signals into 4 by 1 or 2 by 1 pieces.

## 2. Method

### 2.1. Continuous wavelet transforms

If satisfies the different conditions then the wavelet transform of the signal with respect to the function is defined as:

$$X(s, \tau) = \frac{1}{\sqrt{s}} \int_{-\infty}^{\infty} x(t) \psi' \left( \frac{t - \tau}{s} \right) dt \quad (1)$$

where denotes the complex conjugate of, and this is defined in interval of such that, and are the time shift or translation and the scale or dilation of the analysing wavelet respectively.

If we define as

$$\psi_{s, \tau}(t) = \frac{1}{\sqrt{s}} \psi \left( \frac{t - \tau}{s} \right) \quad (2)$$

which means rescaling and shifting by and respectively, then Eq. (1) is expressed as a scalar product of the real signal with the function:

$$X(s, \tau) = \frac{1}{\sqrt{s}} \int_{-\infty}^{\infty} x(t) \psi'_{s, \tau}(t) dt \quad (3)$$

When this function satisfies the admissibility condition, the signal can be found from the wavelet transform by the inverse formula given below:

$$x(t) = \frac{1}{c_{\psi}} \int_{-\infty}^{\infty} \int_{-\infty}^{\infty} X(s, \tau) \psi_{s, \tau}(t) \frac{ds d\tau}{s^2} \quad (4)$$

### 2.2. Convolution Neural Network

The inception of convolutional neural networks (CNNs) can be attributed to the pioneering work of Hubel and Wiesel [13] in the 1960s. Their research on neurons in monkey cortexes, specifically pertaining to local sensitivity and selection of direction, served as the foundation for the development of CNNs. Convolutional Neural Networks (CNNs) utilize techniques such as down sampling, weighted sharing, and local connection to effectively decrease various parameters needed and simplify the neural network's structure. Convolutional Neural Networks (CNNs) have been evaluated in comparison to conventional visual feature extraction techniques, such as the Scale-Invariant Feature Transform (SIFT) and Histogram of Oriented Gradient (HOG). It has been observed that CNNs tend to extract more intricate and comprehensive features. Moreover, Convolutional Neural Networks (CNNs) have the capability to utilize raw images as input, thereby obviating the need for intricate image preprocessing. CNNs are made up of three layers, namely convolutional, pooling, and fully connected layers. The CNN relies heavily on the convolutional layer. This layer's job is to obtain characteristics from input photos or feature maps. Several convolution kernels can be utilised in each convolutional layer to generate various feature maps.

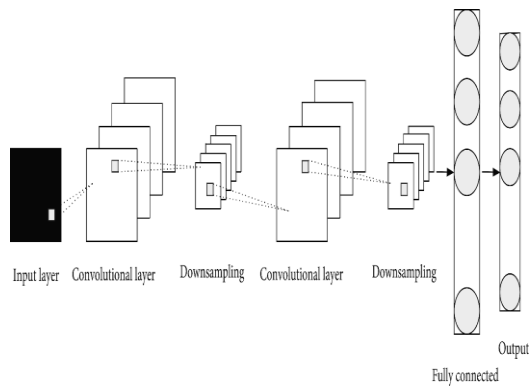


**Figure 1 Convolution neural network architecture**

The convolution layer is calculated in the following manner:

$$x_j^l = f \left( \sum_{i \in M_j} x_i^{l-1} \cdot k_{ij}^l + b_j^l \right) \quad (5)$$

where  $M_j$  is a subset of the input feature maps used to compute  $u_j^l$ ,  $b_j^l$  and  $k_{ij}^l$  are the corresponding offset and convolution kernel,  $f(\cdot)$  referred to as the activation function,  $i^{\text{th}}$  channel of  $j^{\text{th}}$  convolution layer output is denoted by  $x_j^l$ , and the characteristic map of the previous layer output is represented by  $x_i^{l-1}$ , respectively. The majority of the time, a pooling layer will be located between two convolutional layers. The primary focus of this layer is on reducing the dimensionality of the characteristic map while yet preserving some characteristics' scale invariance. Standard pooling algorithms can be broken down into mean pooling and maximum pooling. Pooling effect diagram, as seen in Figure 2.

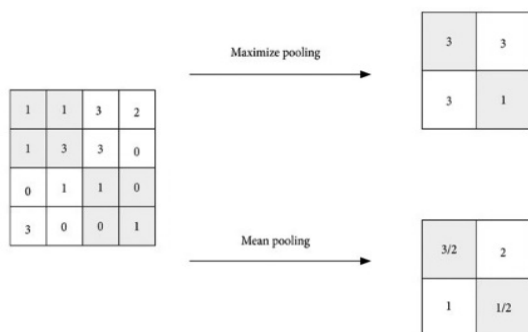


**Figure 2 Pooling effect diagram**

While both pooling and convolution use a sliding window to filter data, the former requires less complicated math. In mean pooling, the average of the values in a set of image pixels is utilized to determine its final value. The approach successfully saves the background of the image. When it comes to preserving an image's texture, max pooling is the best way to go. It does this by using the area's greatest value as the pooled value of that area. The fully connected layer has a function, which is to incorporate many picture maps acquired after the image has been passed via multiple convolution layers and pooling layers to obtain the image's high-layer semantic characteristics for future image classification.

$$|h_{w,b}(x) = f(W^T x) = f \left( \sum_{i=1}^3 W_i x_i + b \right) \quad (6)$$

where  $h_{w,b}(x)$  indicates the output of completely connected layer;  $x_i$  denotes the output of the preceding layer of neurons, that is, fully connected layer's input and  $W_i$ , and  $b$  denote the weight of the connection between neurons and bias, respectively.

### 2.3. Dual channel Convolution Neural Network

In the context of image annotation, it is common for a single image to be associated with multiple annotated words, each of which may correspond to a unique scenario. Several photographs exhibit a high frequency of annotated words that correspond to specific backgrounds.

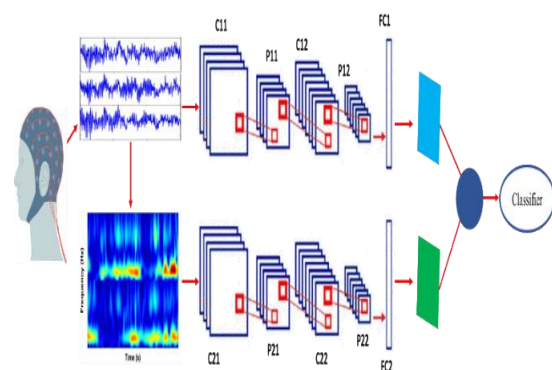


**Figure 3 Structure of Dual Channel Convolution neural network**

In addition, specific segments of the content exhibit

limited visual elements and a reduced lexical density, exemplified by the depiction of a crocodile and a lizard. Improper and adequate training of low-frequency annotated words can result in a low rate of recognition due to unbalanced input data. The present study has devised a DC-CNN model with the aim of enhancing the precision of identification and the efficiency of recognition for words that have been annotated with low frequency (as illustrated in Figure 3).

#### 2.4. Data Augmentation

In contrast to the computer vision domain, which often involves the manipulation of images through rotation, scaling, cropping, distortion, and various data augmentation techniques that primarily employ 2-dimensional data, the electroencephalogram (EEG) signals captured from individual electrodes are typically regarded as 1-dimensional data. There are two primary categories of EEG signal data augmentation methods currently in use, which are referred to as data transformation [14-16] and noise addition [17,18]. The analysis of essential elements of electroencephalogram (EEG) signals demonstrates that EEG signals exhibit distinct features in both the time- and frequency-domains. The present study incorporates a data augmentation (DA) technique, as depicted in Fig. 4 that operates in both the temporal domain and frequency domains, while endeavouring to preserve the fundamental characteristics of the EEG signal.

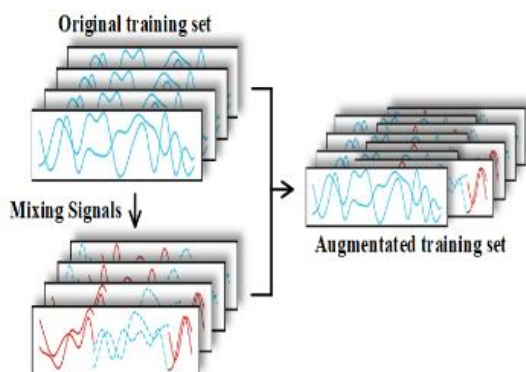


**Figure 4** Generation training set with data augmentation

The present methodology involves the random selection of three samples, namely samples 1, 2, and

3, from a single class. A one-second interval of data from sample 2 was obtained and utilized to substitute the data from sample 1 at the corresponding time position. Fig. 4 illustrates the generation of temporal domain samples. In this investigation, we use band-pass filtering to separate the 8-15 Hz and 14-30 Hz portions of the synthetic time-domain EEG sample into their respective frequency bands. After that, the frequency band of sample 3 is swapped with the one of the synthetic time-domain EEG signal, allowing for the time-frequency EEG signal to be reconstructed with greater ease.

### 3. Results and Discussions

All of the experiments were performed on a computer system configured with processor of an Intel Core i7-1165G7 CPU and a GPU of GeForce RTX 3020Ti. Many international BCI contests have been organized since 2001 to provide experts working in this field with solid data resources and identical detection algorithm criteria. A public data set (2008 BCI Competition IV Dataset 2b [4]) is chosen to assess the performance of the proposed methodology. Figure 5 depicts the data collecting method for this data set. The acquisition of a single EEG signal is separated different stages. The preparation phase of a trial lasts three seconds. The screen displays directional arrow suggestions, which are complemented by an auditory alert. To begin the motor imagery from the third to the sixth second, subjects must follow the on-screen prompts. Following that, the individuals relaxed and awaited the signal to begin the following trial. We intercepted from 3.5 seconds to the end of the sixth second, assuming that the subject was unable to answer when the cue first appeared, for a total of 625 data points.

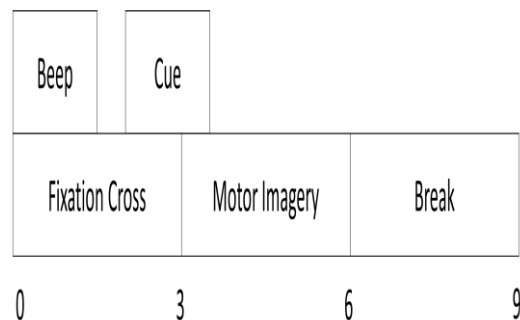


**Figure 5** Timing pattern of proposed model

Figure 6 and 7 depict graphical representations of spectral power comparisons, both pre- and post-signal enhancement. The red line depicts the initial data spectrum, while the blue line illustrates the data spectrum subsequent to augmentation. Additionally, samples depicting the spectrum of C3, Cz, and C4, which are more closely associated with movement, are presented. The study revealed that the augmentation procedure had a negligible impact on the fundamental properties of the initial EEG signal. The proposed approach for digital audio (DA) prioritizes the elevation of the replacement band's energy, while simultaneously preserving a relatively uniform spectral ratio between the signal and its replaced band. The employment of this technique has the potential to enhance the ratio of signal to noise and facilitate a more comprehensive comprehension of the information.

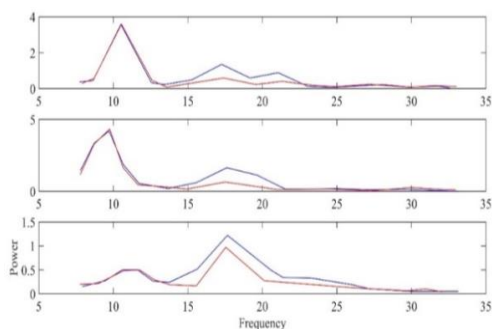


**Figure 6 Power Spectral plots before enhancement**

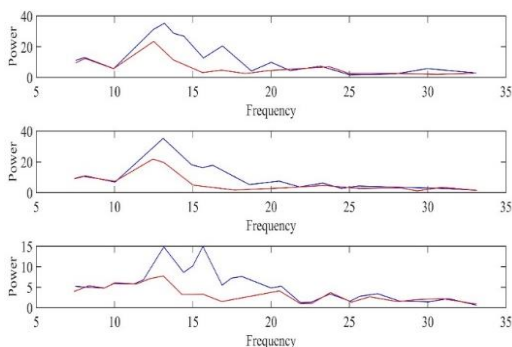


**Figure 7 Power Spectral plots after enhancement**

### 3.1. Determining The Length Of Data Segments

The utilization of data segmentation and overlap techniques is a prevalent approach to augment the quantity of data, thereby leading to a substantial

enhancement in classification accuracy, as indicated by previous research [19]. There is a potential for substantial reduction in resource utilization during network computation procedures. Dimensionality reduction techniques not only decrease the input size, but also minimize the volume of data that needs to be transmitted and stored during the training and inference phases. This leads to enhanced performance and reduced expenses. Consequently, these techniques have the potential to serve as valuable optimization instruments for our purposes. In the present study, a window with a 50% overlap was employed for the sample, indicating that half of the data in each segment appears to be identical to that of the preceding segment. Subsequently, we established the magnitude of the segmentation. Fig. 8 depicts a comparison of accuracy.

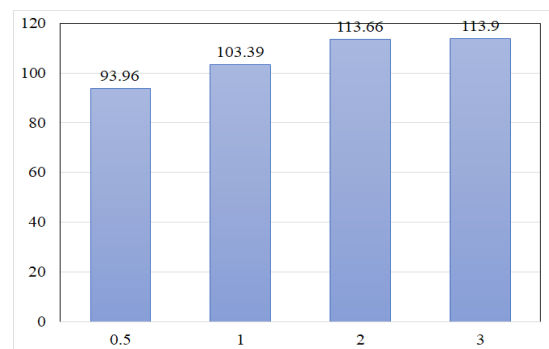


**Figure 8 Comparison of Length Segments**

### 3.2. Performance Of The Proposed Model

The results of proposed method are compared to state of art methods. To demonstrate the efficiency of the proposed method. Particularly, VGGNET with CNN and EEGNET with CNN were compared with proposed model. Here the proposed method retrained two widely cited models (VGGNet and EEGNet) on the same dataset to evaluate their performance. Table 1 shows the comparison results. Moreover, research methods ending in (DA) indicate the use of DA techniques. The proposed method improves accuracy to 99.22%, the highest among the compared methods. Moreover, the proposed data augmentation method can improve accuracy to varying degrees, with average accuracy improvements of up to 5.04% and 11.06% for the individual subject Table 1.

**Table 1** Compared results with EEG Net and VGG Net

Subject No.	Accuracy (%)					
	VGGNet	VGGNet_A	EEGNet	EEGNet_A	Proposed	Proposed_DA
1	79.32	85.36	88.21	91.33	98.15	99.10
2	69.01	77.22	70.35	72.58	95.56	98.99
3	91.11	92.67	92.40	93.14	95.36	98.89
4	68.32	66.12	81.26	85.65	96.42	98.91
5	59.00	70.15	85.77	83.85	94.15	99.69
6	70.32	71.39	73.12	76.98	94.39	99.88
7	82.55	85.73	93.10	98.54	95.3	98.90
8	79.33	88.52	90.73	89.32	96.25	98.92
9	70.74	72.29	91.05	89.99	97.88	99.05
Mean	74.41	78.82	85.11	86.82	95.67	99.91

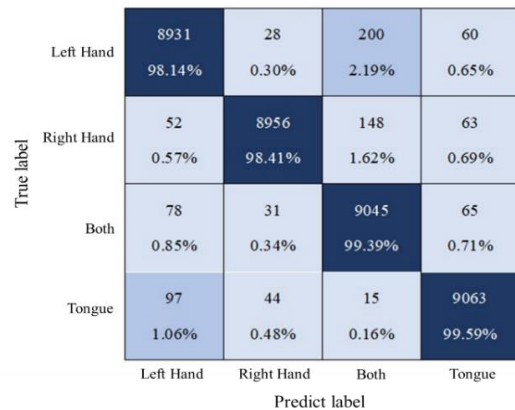


**Figure 10** Confusion matrix represent accuracy of the improved CNN with DA.

### Conclusions

The intricacy of EEG signals often results in low accuracy rates for automatic classification, and limited training data can lead to significant individual differences. An additional concern pertains to the fact that current Convolutional Neural Network (CNN) approaches utilized for Electroencephalogram (EEG) Motor Imagery (MI) classification derive EEG characteristics from a singular domain. The classification of EEG signals is restricted due to the necessity of concurrently decoding temporal, spectral, and spatial information. A hybrid convolutional neural network architecture is proposed in this study, which is founded on the principle of data augmentation. Enhancing the accuracy of EEG motor imagery classification can be achieved by augmenting the input to the CNN with a greater variety of dimensional images, coupled with an increase in the volume of data. The accuracy of a dataset can be improved by determining the appropriate size of the sliding window, as the optimal window size is known to vary across datasets. The utilization of a window size of 2 seconds satisfies the criteria established for the 2008 BCI competition IV 2b dataset. This approach not only diminishes the consumption of computational resources but also yields a satisfactory level of accuracy. The efficacy of the proposed DA technique in enhancing the training accuracy of VGGNet, EEGNet, and the proposed model has been demonstrated. The proposed method for classifying MI-EEG images exhibits an accuracy rate of 99.22%. The method is

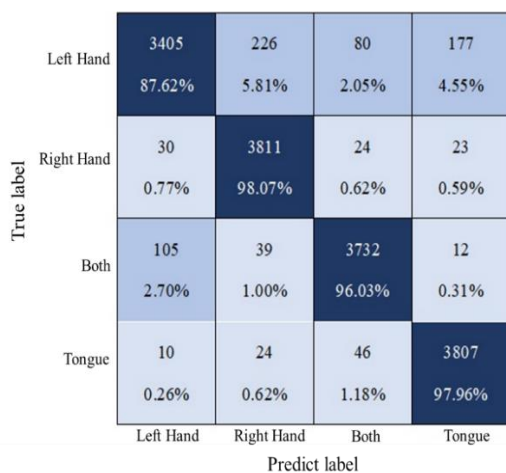


**Figure 9** Confusion Matrix Represent Accuracy of the Improved CNN



enhanced by the implementation of two distinct CNN scales, one for time domain and the other for CWT mapping, resulting in a more comprehensive feature extraction process. The method is enhanced by the implementation of two distinct scales of Convolutional Neural Networks (CNNs) for both time domain and Continuous Wavelet Transform (CWT) mapping, resulting in a more comprehensive feature extraction process. In comparison to alternative approaches, this method exhibits the greatest mean classification precision. The aforementioned findings indicate that the suggested method of data augmentation holds promise in enhancing the efficacy of machine learning models.

### References

- [1]. Roy, Y.; Banville, H.; Albuquerque, I.; Gramfort, A.; Falk, T.H.; Faubert, J. Deep learning-based electroencephalography analysis: A systematic review. *J. Neural Eng.* 2019, 16, 051001.
- [2]. Xie, Y.; Oniga, S. A Review of Processing Methods and Classification Algorithm for EEG Signal. *Carpathian J. Electron. Comput. Eng.* 2020, 13, 23–29
- [3]. Lotte, F.; Bougrain, L.; Cichocki, A.; Clerc, M.; Congedo, M.; Rakotomamonjy, A.; Yger, F. A review of classification algorithms for EEG-based brain–computer interfaces: A 10-year update. *J. Neural Eng.* 2018, 15, 031005.
- [4]. Tangermann, M.; Müller, K.-R.; Aertsen, A.; Birbaumer, N.; Braun, C.; Brunner, C.; Leeb, R.; Mehring, C.; Miller, K.J.; Mueller-Putz, G. Review of the BCI competition IV. *Front. Neurosci.* 2012, 6, 55.
- [5]. Yang, H.; Sakhavi, S.; Ang, K.K.; Guan, C. On the use of convolutional neural networks and augmented CSP features for multi-class motor imagery of EEG signals classification. In *Proceedings of the 2015 37th Annual International Conference of the IEEE Engineering in Medicine and Biology Society (EMBC), Milan, Italy, 25–29 August 2015*; pp. 2620–2623.
- [6]. Tabar, Y.R.; Halici, U. A novel deep learning approach for classification of EEG motor imagery signals. *J. Neural Eng.* 2016, 14, 016003.
- [7]. Xu, G.; Shen, X.; Chen, S.; Zong, Y.; Zhang, C.; Yue, H.; Liu, M.; Chen, F.; Che, W. A deep transfer convolutional neural network framework for EEG signal classification. *IEEE Access* 2019, 7, 112767–112776.
- [8]. Lawhern, V.J.; Solon, A.J.; Waytowich, N.R.; Gordon, S.M.; Hung, C.P.; Lance, B.J. EEGNet: A compact convolutional neural network for EEG-based brain–computer interfaces. *J. Neural Eng.* 2018, 15, 056013.
- [9]. Dai, G.; Zhou, J.; Huang, J.; Wang, N. HS-CNN: A CNN with hybrid convolution scale for EEG motor imagery classification. *J. Neural Eng.* 2020, 17, 016025.
- [10]. Majidov, I.; Whangbo, T. Efficient classification of motor imagery electroencephalography signals using deep learning methods. *Sensors* 2019, 19, 1736.
- [11]. Zhang, R.; Zong, Q.; Dou, L.; Zhao, X. A novel hybrid deep learning scheme for four-class motor imagery classification. *J. Neural Eng.* 2019, 16, 066004. [Google Scholar]
- [12]. Ma, X.; Wang, D.; Liu, D.; Yang, J. DWT and CNN based multi-class motor imagery electroencephalographic signal recognition. *J. Neural Eng.* 2020, 17, 016073.
- [13]. D. H. Hubel and T. N. Wiesel, “Receptive fields and functional architecture of monkey striate cortex,” *Journal of Physiology*, vol. 195, no. 1, pp. 215–243, 1968.
- [14]. Pei, Y.; Luo, Z.; Yan, Y.; Yan, H.; Jiang, J.; Li, W.; Xie, L.; Yin, E. Data Augmentation: Using Channel-Level Recombination to Improve Classification Performance for Motor Imagery EEG. *Front Hum Neurosci* 2021, 15, 645952.
- [15]. Kim, S.K.; Kirchner, E.A.; Stefes, A.; Kirchner, F. Intrinsic interactive reinforcement learning—Using error-related potentials for real world human-robot interaction. *Sci. Rep.* 2017, 7, 17562.
- [16]. Le Guennec, A.; Malinowski, S.; Tavenard, R. Data augmentation for time series classification using convolutional neural networks. In *Proceedings of the ECML/PKDD Workshop*



on Advanced Analytics and Learning on  
Temporal Data, Riva del Garda, Italy, 19  
September 2016.

- [17]. Wang, F.; Zhong, S.-h.; Peng, J.; Jiang, J.; Liu, Y. Data augmentation for eeg-based emotion recognition with deep convolutional neural networks. In Proceedings of the International Conference on Multimedia Modeling, Bangkok, Thailand, 5–7 February 2018; pp. 82–93.
- [18]. Li, Y.; Huang, J.; Zhou, H.; Zhong, N. Human emotion recognition with electroencephalographic multidimensional features by hybrid deep neural networks. *Appl. Sci.* 2017, 7, 1060.
- [19]. Freeman, W.J. Origin, structure, and role of background EEG activity. Part 2. Analytic phase. *Clin. Neurophysiol.* 2004, 115, 2089–2107.